6G Channel Measurement in Urban, Dense Urban Scenario and Massive Ray-Tracing-Based Coverage Analysis at 7.5 GHz

Hyunjun Yang*, Seungwoo Bang*, Hooyoung Kim*, Sunghyun Kim†, Yusuk Sung†,
Kyujin Park†, Seongkwan Kim†, Jungsuek Oh*,
*Institute of New Media and Communications, Dept. of Electrical and Computer Engineering,
Seoul National University, Seoul, South Korea. e-mail: guswns6217@snu.ac.kr, jungsuek@snu.ac.kr
†Institute of Convergence Technology, KT Corporation, Seoul, South Korea. e-mail: sh85.kim@kt.com

***Abstract*—As demands for 6G communication continue to grow beyond 5G-Advanced and 5G capabilities, interest in the upper midband is increasing. However, channel model measurement studies at the upper midband are still limited, and measurement-based channel modeling across diverse propagation scenarios is essential for extending to 6G. Therefore, in this paper, the authors perform a measurement-based close-in path loss (PL) model fitting for Line of Sight (LOS) and Non-Line of Sight (NLOS) in urban and dense urban scenarios, presenting the PL exponent and shadow fading parameters. Measurements were conducted with a channel sounder at 7.5 GHz with 200 MHz bandwidth, achieving maximum T-R separation distances of 306 and 288 meters in Urban Macrocell (UMa) and Urban Microcell (UMi), respectively. Furthermore, a state-of-the-art (SOTA) 6G ray-tracing engine was used to perform simulations in a massive UMi scenario, ensuring the reliability of the measurement results. Finally, in response to the need to maintain 7.5 GHz coverage similar to that at 3.5 GHz, we propose the required gain for similar coverage in dense urban environments.**

***Index Terms*—6G Channel Measurement, Urban, Dense Urban, Channel Sounder, Ray-tracing, 6G, Coverage Analysis.**

I. Introduction

In the upcoming 6G era, research on wireless communications in new frequency bands is becoming crucial. To meet these demands, the upper mid-band (7–24 GHz) has been identified as a key candidate for 6G deployment, bridging the spectral gap between the sub-6 GHz bands used in 5G and the mmWave bands above 24 GHz. At world radiocommunication conference (WRC)-23, the 4.4–4.8 GHz, 7.125–8.4 GHz, and 14.8–15.35 GHz bands were discussed as strong candidates for future international mobile telecommunications (IMT)-2030 allocations. Additionally, each ITU region has been tasked with completing research on its assigned frequency bands by the upcoming WRC-27. Among them, ITU Region 3, which includes South Korea, will assess the feasibility of 6G deployment in the 7.125–8.4 GHz band.

Expanding into new frequency bands requires research and development across various fields, including radio frequency (RF) devices [1]–[3] and beam management [4], to accommodate new application scenarios. In the mmWave band, despite efforts such as reconfigurable intelligent surfaces (RIS) [1] to overcome its limited coverage, the fundamental coverage constraints in mmWave channels could not be fully addressed. As a result, the transition from 5G-Advanced to preparations for 6G has begun. Clearly, 6G must learn from the experiences of the mmWave band and conduct a thorough channel analysis of the upper mid-band to ensure the success of innovative 6G applications such as RIS, integrated sensing and communication (ISAC), and vehicular-to-vehicular (V2V) communication. However, several studies [5], [6] have pointed out that existing 3GPP frequency-dependent models [7], which cover a wideband range from 0.5 to 100 GHz, cannot accurately capture the channel characteristics of the upper mid-band. For this reason, recent channel modeling studies have focused on the upper mid-band across various scenarios, such as urban [8], indoor [9], and outdoor-to-indoor [5] environments, to characterize its channel properties more accurately. Accordingly, this study also examines channels in diverse urban environments.

Furthermore, in 6G research, coexistence with 5G, such as the sharing of spectrum resources, is one of the key areas of interest. From a coverage perspective, coexistence analysis requires multiple campaigns across the frequency bands of interest, conducted under the same conditions, including the test location and equipment. However, in the currently commercialized 5G 3.5 GHz band, only licensed signals can be transmitted under strict government authorization, and campaigns require the costly time and budget. Consequently, many studies [1], [10] have developed high-performance ray-tracing simulators as an alternative to campaigns. In this study, ray-tracing is also utilized to analyze the coverage of both the 5G and upper mid-band.

The main contributions and insights revealed by our survey are as follows.

- **6G UMi & UMa propagation measurements and PL models at 7.5 GHz upper mid-band:** This study conducts an in-depth analysis of the channel characteristics in the 6G frequency candidate designated by the ITU and compares them with the 3GPP channel model to examines the potential for extending the 3GPP model to the upper mid-band.

ICC 2025 - IEEE International Conference on Communications | 979-8-3315-0521-9/25/$31.00 ©2025 IEEE | DOI: 10.1109/ICC52391.2025.11161469

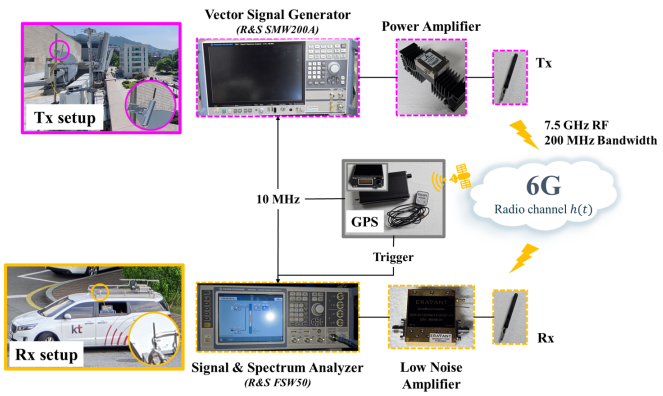

Fig. 1: Channel Sounding Setup.

- **High-fidelity channel modeling and the establishment of deterministic channels using 6G SOTA ray-tracing:** We conduct 6G state-of-the-art (SOTA) ray-tracing simulation with high accuracy based on the image method in massive UMi environment, enabled by GPU-based parallel processing [1]. Ray-tracing simulations in the massive UMi scenario are used to evaluate the reliability of measurement data while also establishing a deterministic channel model.
- **A ray-tracing-based coverage expansion strategy in the upper mid-band:** We utilized our self-developed massive ray-tracing simulation to obtain coverage data for the 5G 3.5 GHz channel, where measurements are restricted. The system parameters derived from the simulation results were used to compare the coverage of 5G 3.5 GHz and 7.5 GHz upper mid-band. As a result, we calculated the additional gain to achieve the same coverage as 3.5 GHz in a dense urban environment. The findings offer a pioneering guide for coverage expansion strategies to support the 6G establishment.

The remainder of this paper is organized as follows. First, we introduce the channel sounder setup and measurement scenarios in UMa and UMi. Next, we present the channel model fitting parameters based on measurement results and establish reliability through ray-tracing validation. Finally, we propose a downlink (DL) coverage analysis using ray-tracing, comparing 7.5 to 3.5 GHz to outline approaches for achieving comparable coverage.

II. 6G Channel Measurement

This session introduces the 6G channel sounding setup, and scenarios. Measurements were conducted via a drive test, as shown in Fig. 1, at Seoul National University (SNU) Building 71 for the UMa channel and the KT Gwanak Office for the UMi channel, reflecting dense urban characteristics. Scenarios were categorized into UMi and UMa based on the 3GPP Inter-site Distance (ISD) classification [7].

TABLE I: Channel Sounding Parameters

Parameter	Value
Sampling rate at Tx [MHz]	240
Sampling rate at Rx [MHz]	250
Sounding sequence duration [μs]	50
Measurement time [ms]	5
Sounding waveform	Frank-Zadoff-Chu sequence

A. Channel Sounder Setup

The measurements were conducted based on instrument utilizing the principles of time-domain channel sounding, as mentioned in [11]. The block diagram of the channel sounder system used at the transmitter (Tx) and receiver (Rx) is shown in Fig. 1. Time synchronization between the Tx and Rx was achieved using a GPS module to enable channel sounding measurements over long distances without a cable connection. A 10 MHz reference clock, derived from the GPS module's 1 pps signal, was applied to both the Tx and Rx. This reference clock also ensured coherent triggering at the Rx. At the Tx end, a vector signal generator (R&S SMW200A) produces a 200 MHz bandwidth channel sequence at an RF frequency of 7.5 GHz with a sampling rate of 240 MHz. The signal is then amplified using a power amplifier (PA) with a 35 dB gain and transmitted via a half-dipole antenna. At the Rx side, the received signal is captured with the same omnidirectional antenna as the Tx and amplified by a 40 dB gain low-noise amplifier (LNA) to enhance the dynamic range. Finally, the time-domain IQ signal is recorded in real time at a 250 MHz sampling rate using a signal and spectrum analyzer (R&S FSW50). The channel sounding parameters are summarized in Table I. The selected channel sounding sequence is the Frank-Zadoff-Chu (FZC) sequence, a type of constant amplitude zero autocorrelation (CAZAC) waveform, with a 50 μs duration. Owing to its good correlation properties, the FZC sequence is widely used in LTE and 5G NR applications, such as DL synchronization and uplink (UL) random access [12].

B. Measurement Scenario

1) UMa Scenario at SNU Building 71: The measurement site for UMa scenario was selected at SNU Building 71, where the ISD is 150 to 400 meters, according to a website [13] provided by the Korean government. As shown in Fig. 2, the Tx was installed beside the 5G BS at a height of 15 meters above the ground and downtilted by 15 degrees to align with the downtilt of the 5G BS. The Rx was mounted vertically on the roof of a car at a height of 2 meters above the ground. Additionally, the Rx route has flat terrain, minimizing interference from the surrounding environment. To eliminate the impact of the car's mobility, measurements were conducted only after the car had come to a complete stop. For both UMa and UMi, LOS is defined as the Rx point within the Tx's boresight, and NLOS is defined as the case where there is no clear direct path between the Tx and Rx, as in [14].

2) UMi Scenario at KT Gwanak Office: The UMi scenario was conducted at the KT Gwanak Office, where two 5G BSs

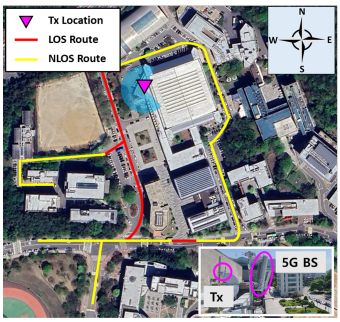

Fig. 2: UMa Measurement Scenario.

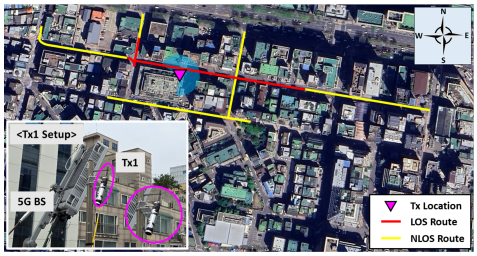

(a)

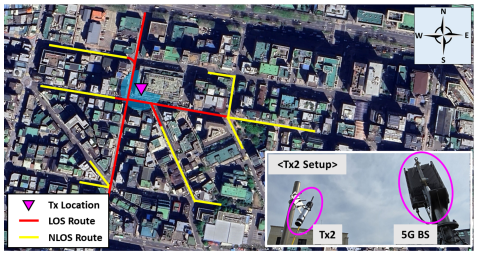

(b)

Fig. 3: UMi Measurement Scenario. (a) Tx1 setup and measurement routes, and (b) Tx2 setup and measurement routes.

are installed and labeled as Tx1 and Tx2, as shown in Fig. 3. The KT Gwanak Office is located in a densely populated residential urban area, with an ISD of approximately 30 to 120 meters, designed for a UMi scenario in a 5G network. The measurement campaign was performed at the location of each 5G BS, as depicted in Fig. 3. The heights of Tx1 and Tx2 are 19 and 22 meters above the ground, respectively. The downtilt angles of both Txs are 15 degrees.

III. Omni-directional Path Loss Model and Reliability Verification using Ray-tracing

This section introduces the measurement data processing and presents the results of the close-in (CI) and alpha-beta-gamma (ABG) path loss (PL) models. Furthermore, the reliability of the measurement results is verified by comparison with ray-tracing simulations.

A. Data Processing

Before conducting channel measurements, back-to-back calibration was performed to eliminate cable loss and system impairment, as referenced in [6], [10], [11]. For each measurement point, the channel sounder records 100 channel impulse response (CIR) snapshots. To mitigate the effects of small-scale fading, the captured CIR snapshots were incoherently averaged to obtain the average power delay profile (APDP). The APDP can be defined as

$$P(\tau) = \frac{1}{N_{\text{snapshots}}} \sum_{i=1}^{N_{\text{snapshots}}} |h_i(\tau)|^2 . \tag{1}$$

where $h_i(\tau)$ is the CIR at the i-th snapshot, and $N_{\text{snapshots}}$ is the number of recorded snapshots. Consequently, the PL was obtained by accumulating the local maxima in the APDP. Note that the average value of PL, measured multiple times at the same point without the antenna gain, is used for fitting the PL model.

B. Path Loss

The CI free-space reference distance PL model was used for PL modeling and can be expressed as

$$PL(f,d)\,[\text{dB}] = FSPL(f, 1\,\text{m}) + 10n \log_{10}\left(\frac{d}{1\,\text{m}}\right) + X_\sigma \tag{2}$$

where f is the frequency, d is the T-R separation distance, n is path loss exponent (PLE), X is the zero-mean Gaussian random variable with the standard deviation of shadow fading, which is indicated as σ in dB. $FSPL(f, 1\,\text{m})$ is the free space PL in dB at the reference distance of 1 m at frequency f, and is represented as

$$FSPL(f, 1\,\text{m})\,[\text{dB}] = 20 \log_{10}\left(\frac{4\pi f}{c}\right) \tag{3}$$

where c is the speed of light. CI PL model fitting parameter is obtained by the least-squares regression analysis.

The ABG model, used in 3GPP as an alternative to the CI model, is detailed in [14]. However, as noted in many studies, including [14], the ABG model lacks a physical basis and is only valid for the measurement distances where the data was collected. Therefore, many channel studies [6], [8], [10], [14] have chosen the CI PL model, which is physically based and can be easily applied to 3GPP models.

1) UMa Scenario at SNU Building 71: In the UMa environment, a total of 70 and 57 measurement data points were obtained for LOS and NLOS, respectively. The T-R separation distance ranges from 35 to 190 meters in LOS and from 45 to 306 meters in NLOS. The results for UMa scenario are shown in red and blue colors in Fig. 4. The authors present the omnidirectional CI PL model parameters for the UMa environment, with LOS values of $n = 2.03, \sigma = 4.71$. These results are consistent with previous studies [7], [10], [14], [15], which report LOS PLEs between 2.0-2.1 and σ values between 2-5, regardless of frequency and measurement environment, owing to its dominant direct path. For NLOS, the parameters

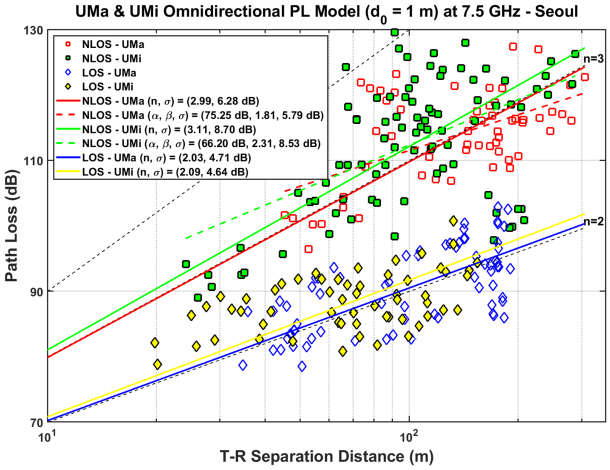

Fig. 4: Omnidirectional PL Model in UMa and UMi Scenario.

Fig. 5: CAD Model for UMi Scenario.

are $n = 2.99, \sigma = 6.28$, as shown in Fig. 4. In the ABG model, the fitted σ is reduced by less than 1 dB compared to the CI model, indicating no significant difference. This suggests that, as in the 5G band [14], the CI model, which provides greater physical insight, is likely to be preferred over the ABG model, even in the upper mid-band.

2) UMi Scenario at KT Gwanak Office: For the UMi environment, 58 and 90 data points were collected for LOS and NLOS, respectively, with T-R separation distances ranging from 20 to 154 meters in LOS and from 24 to 288 meters in NLOS. In the UMi environment, owing to dense and tall buildings, the T-R separation distance range for LOS is shorter than in the UMa environment. Additionally, due to the rich scattering paths, the maximum measurable distance in NLOS, where signals can be distinctly separated from the noise of the spectrum analyzer, is shorter than that in UMa. The results in the UMi environment are represented by the green and yellow colors in Fig. 4. The fitting parameters of the LOS CI PL model were $n = 2.09, \sigma = 4.64$, similar to the values mentioned earlier. Meanwhile, the NLOS CI PL fitting parameters were $n = 3.11, \sigma = 8.70$, experiencing greater propagation loss and σ than in UMa. These results can be interpreted from a geometric optics perspective. Rays from the Tx undergo more interactions with buildings, including

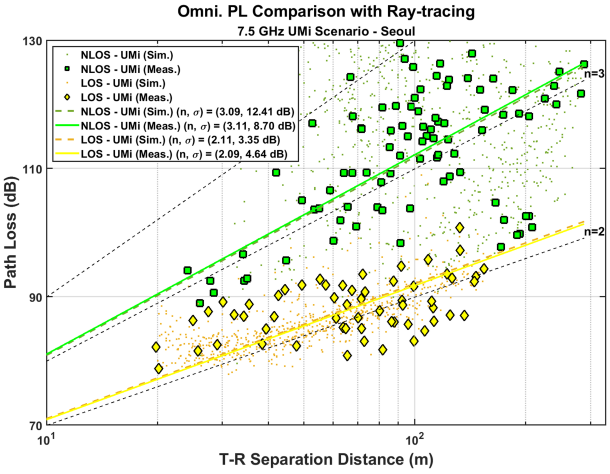

(a)

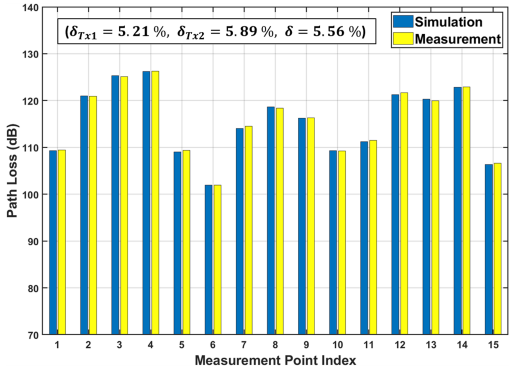

(b)

Fig. 6: PL Result Comparison with Ray-tracing in UMi Measurement Scenario. (a) CI PL model for both measurement and ray-tracing, and (b) PL values at certain NLOS measurement points. δ denotes the RMSPE between the measurement and ray-tracing for all 90 NLOS points, i.e.,. $\delta = \sqrt{\frac{1}{m}\sum_{i=1}^{m}\left(\frac{\mathrm{PL}_{meas}-\mathrm{PL}_{sim}}{\mathrm{PL}_{sim}}\right)^2} \times 100\,\%$ where m is the number of points.

reflections, diffractions, and scattering, creating numerous multipaths that increase σ and result in higher propagation loss. In the UMi scenario, the ABG model, similar to the UMa scenario, showed no significant difference compared to the CI model.

Consequently, the measurement results in the UMi and UMa environments showed similar PL model parameters to those in the 3GPP UMi - Street Canyon and UMa scenarios [7], [15], respectively, thus confirming the possibility of extending the 3GPP model to the upper mid-band. The authors noted the importance of accurate channel modeling at the 7.5 GHz upper mid-band for 6G, given that most prior channel measurements have primarily focused on frequencies below 6 GHz and in the mmWave band [10], [14], [16], while recent analyses are increasingly being conducted in the 6G upper mid-band [5], [6], [8], [9]. Therefore, to enhance the reliability of the PL data

analyzed in this paper, the authors compared the measured data with SOTA ray-tracing simulation [1], as commonly done in many channel measurement analyses such as in [1], [10], [17].

C. Comparison with Ray-tracing Simulation

For the comparison, we used the self-developed SNU 3D Ray-tracer, which features high accuracy based on the image method and fast computation through GPU acceleration [1]. The performance of this SOTA ray-tracer, which includes RIS analysis not supported by many commercial programs, was proven in [1] by accurately predicting both coverage hole and RIS coverage enhancement in multipath-rich environments, showing high correlation with field trials. In this paper, the validity of the measurement results is verified through two methods: comparing the root mean square percentage error (RMSPE) between the measured and simulated PL, and comparing the simulation-fitted PLE with the measured values.

Since the measurements in UMa and UMi were conducted using the same setup, and the propagation characteristics of the UMi measurement scenario are more complex than those of UMa, the simulation analysis was conducted in the UMi scenario. The 3D CAD model of the UMi scenario surrounding the KT Gwanak Office was shown in Fig. 5. The 3D CAD model was first created by downloading polygons, including building shapes and heights, from Open Street Map. Subsequently, additional building meshes were completed using V-World, a 3D mapping service provided by the Korean government.

For the ray-tracing simulation, the authors set the material properties (relative permittivity, conductivity) of the ground and buildings to (3, 0.0241) and (5.31, 0.1666), corresponding to ITU-R's dry ground and concrete as in [1], respectively. As shown in Fig. 5, a total of 3,000 Rx points were uniformly distributed along the road where the driving test was conducted. The heights and downtilt angles of the Tx and Rx were set identical to those in the measurements, and the radiation patterns were configured as a 2.15 dBi half-dipole radiation pattern from [18] and an isotropic pattern, respectively. Additionally, the maximum number of bounces is set to 6, including 6 reflections and 1 diffraction.

Note that when fitted CI model parameter with simulated PL values, only values within the T-R separation distance range from measurements and not exceeding the maximum measured PL value were included. Since these simulations were conducted separately for Tx1 and Tx2, there is no interference between the Tx units in the simulated PL values. The CI PL model fitting results for LOS and NLOS points showed very similar outcomes to the measurement data, with $n = 2.11, \sigma = 3.35$ for LOS, and $n = 3.09, \sigma = 12.41$ for NLOS, as shown in Fig. 6(a). Additionally, as depicted in Fig. 6(b), the authors calculated the RMSPE by comparing simulated PL values with measured PL values at the 90 NLOS points measured in UMi. Fig. 6(b) displays only a subset of the NLOS points where the simulated and measured PL values closely match. Across all NLOS points, δ is 5.56, and the separately calculated values for Tx1 and Tx2, δ_{Tx1} and δ_{Tx2}, are 5.21 and 5.89, respectively. The authors confirmed the reliability of the measurement data by verifying its similarity to the ray-tracing results through the above two analyses.

TABLE II: DL Link Budget Simulation Setup in UMi Scenario

Etc. Parameter	Center frequency [GHz]	3.5	7.5
	Bandwidth [MHz]	100	
	SNR [dB] at edge	5	
	Edge coverage probability [%]	86	
	σ [dB]	7.82	
	Interference margin [dB]	5	
	Shadowing margin [dB]	8.45	
	Active BS locations	7 actual 5G BS	
Transmitter end	BS HPBW in Azi., Ele. [deg]	65, 6	
	BS antenna gain [dBi]	16.00	
	BS output power [dBm]	33.00	
	BS EIRP [dBm]	49.00	
Receiver end	UE antenna gain [dBi]	0	
	UE noise figure [dB]	10	
	Receiver sensitivity [dBm]	-79.00	
Maximum allowable path loss (MAPL) [dB]		114.55	114.55

IV. Ray-tracing-based Down Link Coverage Analysis with 5G NR

As previously mentioned, mobile network operators, reflecting on the failure of the 5G mmWave band, aim to achieve a balance between coverage and capacity in 6G. This goal shifts their focus toward a new topology that ensures a single 6G BS provides coverage similar to 5G, unlike the 5G topology, which addressed limited coverage by deploying a denser BS network. Thus, in Section IV, we analyze the DL coverage for 5G at 3.5 GHz and 6G at 7.5 GHz in the dense urban scenario shown in Fig. 5, and examine the gain required for 6G to achieve the same coverage as 5G.

First, the DL link budget calculation was conducted as shown in Table II. Note that the SNR, edge coverage probability, and UE noise figure were selected based on [6], as these parameters are vendor specifications that are not publicly available. The shadowing margin is calculated using erfc(), based on the edge coverage probability and σ from the 3GPP UMi Model. Additionally, the BS configuration is designed based on the second synchronization block (SSB) beam pattern of KT Corporation's 5G BSs. Note that the cell is defined as the area not exceeding the MAPL. Additionally, for the purpose of comparing coverage with 3.5 GHz, the 7.5 GHz cell is defined as the area within the 3.5 GHz cell.

In Fig. 7, κ represents the combined simulation results for the seven triangular locations corresponding to the actual 5G BS locations shown in Fig. 7(a). Furthermore, Figs. 7(a)-(c) show the coverage simulations for the pink triangular location. As shown in Fig. 7(a), under the setup in Table II, the 7.5 GHz cell covers 63 % of the 3.5 GHz cell. With additional gain, κ increases as depicted in Fig. 7(d), exceeding 90 % at 8.2 dB, with the growth rate saturating beyond 10 dB. Since

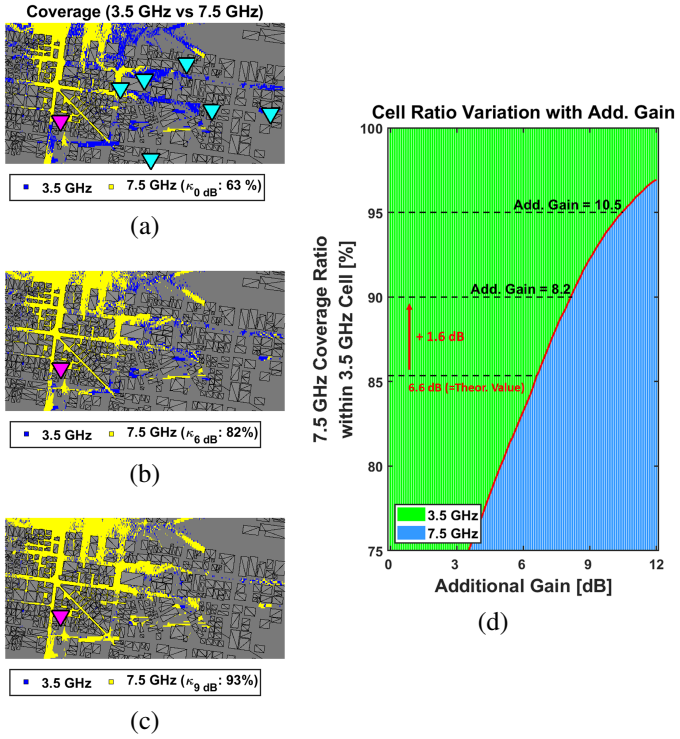

Fig. 7: Cell Ratio Variation with Additional Gain at 7.5 GHz. (a-c) 0, 6, 9 dB gain, and (d) histogram of cell ratio with additional gain. κ denotes the cell ratio.

90 % coverage probability is generally used as the threshold for cell design, the authors analyzed 8.2 dB as the gain margin for the dense urban environment. This is noteworthy as it is greater than the 6.6 dB propagation loss due to the frequency difference, reflecting the differing multipath channel characteristics of 3.5 and 7.5 GHz in dense urban areas. Future research requires an analysis that incorporates the cost of RF units, such as PA, signal processing methods including digital predistortion (DPD), and antenna elements as constraints to achieve the additional gain.

V. Conclusion

We conducted a channel measurement at 7.5 GHz, part of the 6G upper mid-band, in both UMa and UMi (dense urban) scenarios and validated the PL analyses through ray-tracing simulation. The fitting results of the CI PL model for NLOS showed $n = 2.99, \sigma = 6.28$ in UMa and $n = 3.11, \sigma = 8.70$ in UMi, confirming the similarity to the 3GPP model and supporting the potential for extending the 3GPP model to the upper mid-band. Additionally, we designed the additional gain of the 6G system required for a 6G single isolated cell to achieve 5G coverage using the SOTA ray-tracer. It was determined that an additional gain of 8.2 dB is required to achieve 90 % of the 5G coverage in the dense urban area.

Acknowledgment

This work was supported in part by KT Corporation, and in part by the Institute of Information and Communications Technology Planning and Evaluation (IITP) Grant funded by the South Korea Government [Ministry of Science and ICT (MIST)] (Advanced and Integrated Software Development for Electromagnetic Analysis) under Grant 2019-0-00098. The authors also express gratitude to Rohde and Schwarz for their support throughout the channel measurement campaign.

References

[1] H. Yang, S. Kim, H. Kim, S. Bang, Y. Kim, S. Kim, K. Park, D. Kwon, and J. Oh, "Beyond limitations of 5g with ris: Field trial in a commercial network, recent advances, and future directions," *IEEE Communications Magazine*, 2023.

[2] B. Kim, J. Jung, S. Yun, H. Kim, and J. Oh, "Heterogeneous metasurface empowering proximate high-permittivity ceramic cover for a 5g dual-band millimeter-wave smartphone," *IEEE Transactions on Antennas and Propagation*, 2024.

[3] H. Kim, J.-W. Lee, J. Wang, M.-S. Kim, H.-R. Kim, and J. Oh, "Waveguide-thru closed-form characterization of anisotropic polymer network liquid-crystal for mmwave reconfigurable rf devices," *IEEE Transactions on Antennas and Propagation*, 2024.

[4] K. Kim, J. Song, J.-H. Lee, S.-H. Hyun, and S.-C. Kim, "Spatial distribution based beam design for millimeter wave v2v communication systems," *IEEE Transactions on Communications*, 2024.

[5] M. Na, J. Lee, G. Choi, T. Yu, J. Choi, J. Lee, and S. Bahk, "Operator's perspective on 6g: 6g services, vision, and spectrum," *IEEE Communications Magazine*, vol. 62, no. 8, pp. 178–184, 2024.

[6] H. Miao, J. Zhang, P. Tang, L. Tian, X. Zhao, B. Guo, and G. Liu, "Sub-6 ghz to mmwave for 5g-advanced and beyond: Channel measurements, characteristics and impact on system performance," *IEEE Journal on Selected Areas in Communications*, vol. 41, no. 6, pp. 1945–1960, 2023.

[7] *Study on Channel Model for Frequencies From 0.5 to 100 GHz (Release 15)*. document 3GPP TR 38.901, 3GPP, Dec. 2017.

[8] D. Shakya, M. Ying, T. S. Rappaport, P. Ma, I. Al-Wazani, Y. Wu, Y. Wang, D. Calin, H. Poddar, A. Bazzi *et al.*, "Urban outdoor propagation measurements and channel models at 6.75 ghz fr1 (c) and 16.95 ghz fr3 upper mid-band spectrum for 5g and 6g," *arXiv preprint arXiv:2410.17539*, 2024.

[9] R. Bomfin, A. Bazzi, H. Guo, H. Lee, M. Mezzavilla, S. Rangan, J. Choi, and M. Chafii, "An experimental multi-band channel characterization in the upper mid-band," *arXiv preprint arXiv:2411.12888*, 2024.

[10] J.-H. Lee, J.-S. Choi, and S.-C. Kim, "Cell coverage analysis of 28 GHz millimeter wave in urban microcell environment using 3-D ray tracing," *IEEE Transactions on Antennas and Propagation*, vol. 66, no. 3, pp. 1479–1487, 2018.

[11] M. Schmieder, W. Keusgen, M. Peter, S. Wittig, T. Merkle, S. Wagner, M. Kuri, and T. Eichler, "Thz channel sounding: Design and validation of a high performance channel sounder at 300 ghz," in *2020 IEEE wireless Communications and networking Conference workshops (WCNCW)*. IEEE, 2020, pp. 1–6.

[12] A. Zaidi, F. Athley, J. Medbo, U. Gustavsson, G. Durisi, and X. Chen, *5G Physical Layer: principles, models and technology components*. Academic Press, 2018.

[13] M. of Science and S. K. ICT, "Spectrum map - south korea," https://spectrummap.kr/index.do.

[14] T. S. Rappaport, G. R. MacCartney, M. K. Samimi, and S. Sun, "Wide-band millimeter-wave propagation measurements and channel models for future wireless communication system design," *IEEE transactions on Communications*, vol. 63, no. 9, pp. 3029–3056, 2015.

[15] N. Docomo *et al.*, "5g channel model for bands up to100 ghz," Technical report, Tech. Rep., 2016.

[16] G. R. Maccartney, T. S. Rappaport, M. K. Samimi, and S. Sun, "Millimeter-wave omnidirectional path loss data for small cell 5g channel modeling," *IEEE access*, vol. 3, pp. 1573–1580, 2015.

[17] B. Ao, J. Yang, R. Han, D. Fei, L. Wang, N. Wang, Z. Song, and B. Ai, "Channel measurements and sparsity analysis for air-to-ground mmwave communications," in *ICC 2024-IEEE International Conference on Communications*. IEEE, 2024, pp. 1909–1914.

[18] C. A. Balanis, *Antenna theory: analysis and design*. John wiley & sons, 2016.